Electronic Supplementary Material (ESI) for RSC Advances.

Supporting Information

Integration of a silk fibroin based film as luminescent down-shifting layer in ITO-free organic solar cells

Mario Prosa,[a] Anna Sagnella,[b] Tamara Posati,[c] Marta Tessarolo,[a] Margherita Bolognesi,[c] Susanna Cavallini,[a] Stefano Toffanin,[a] Valentina Benfenati,[b] Mirko Seri,*[b] Giampiero Ruani,[a] Michele Muccini[a] and Roberto Zamboni[b]*

[a)] Consiglio Nazionale delle Ricerche (CNR) – Istituto per lo Studio dei Materiali Nanostrutturati (ISMN), Via P. Gobetti, 101, 40129, Bologna, Italy.

[b)] Consiglio Nazionale delle Ricerche (CNR) - Istituto per la Sintesi Organica e la Fotoreattività (ISOF), Via P. Gobetti, 101, 40129, Bologna, Italy.

[c)] Laboratory MIST E-R, Via P. Gobetti, 101, 40129, Bologna, Italy.

Experimental details on solubility and thermal tests of DMSO doped SF films

A glass substrate coated with DMSO doped SF (thickness ~ 400 nm) was soaked in 0.01 M HCl solution (pH = 2) for 60 seconds to simulate the deposition of HC-PEDOT:PSS solution onto SF film. The resulting wet film was firstly rinsed with distilled water to remove eventual residues of HCl solution, dried with a stream of Ar gas and then annealed at 120°C for 20 minutes to simulate the thermal treatment performed on HC-PEDOT:PSS layer.

Table S1. Characterization of DMSO doped SF films after solubility and thermal tests. The reported data are averaged over 5 samples.

DMSO doped SF film	**Thickness** (nm)	**Surface roughness**[a] (nm)
Pristine	380	2
After acidic treatment	380	1.5
After acidic and thermal treatment	380	1.5

[a] Results obtained by profilometer measurements at 50 µm/s scan rate over 2 mm x 2 mm surface.

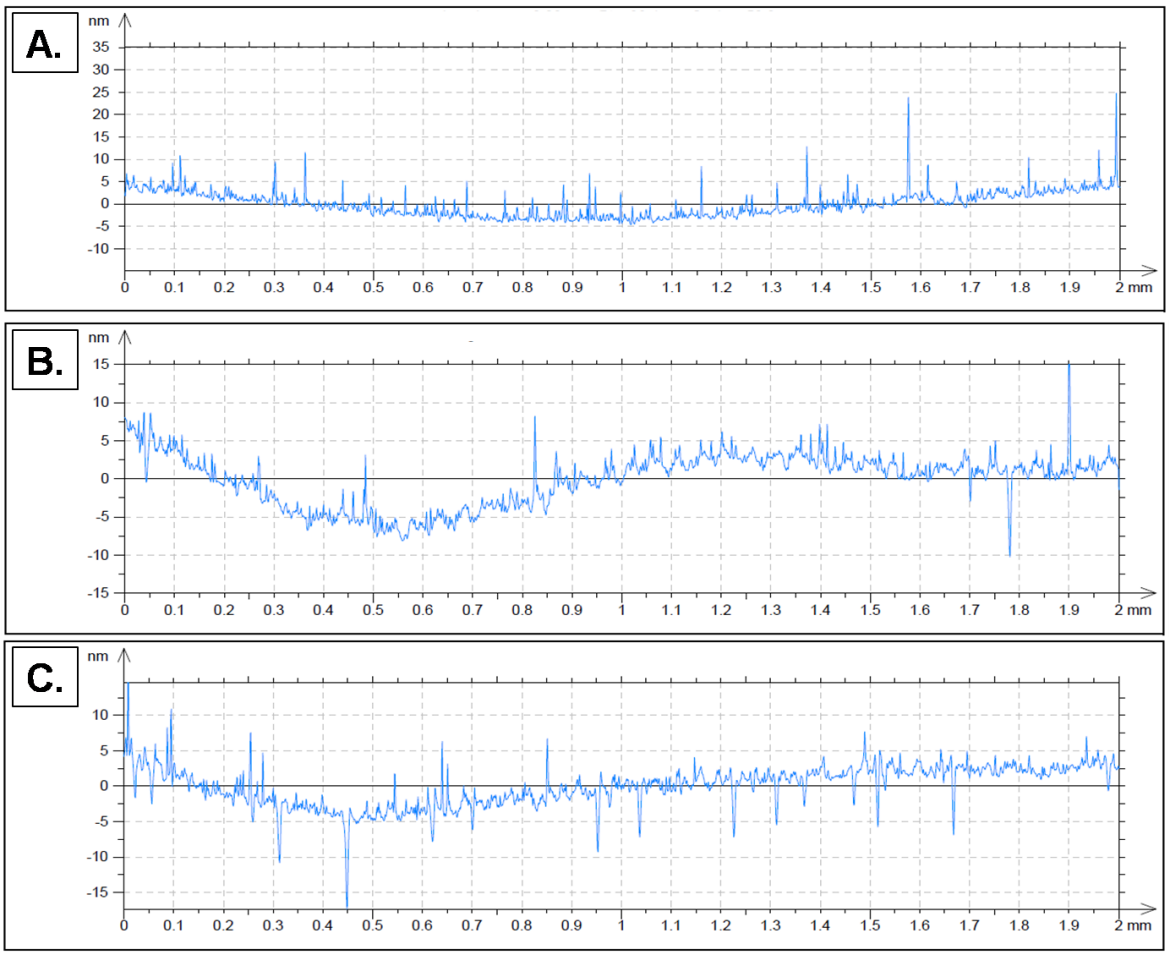

Figure S1. Mean surface profile recorded at 50 µm/s scan rate over 2 mm x 2 mm surface of pristine (A), acidic treated (B) and, acidic and thermal treated (C) DMSO doped SF film. Each mean profile is averaged over 10 scans.

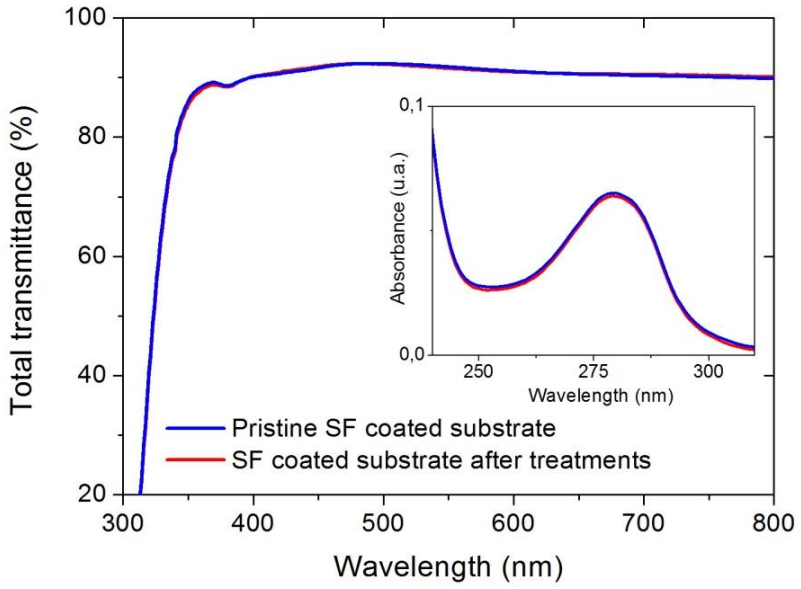

Figure S2. Total transmittance spectrum of DMSO doped SF film casted on glass substrate, before (blue trace) and, after acidic and thermal treatments (red trace). In the inset graph, the absorbance spectra of the relative SF films deposited on quartz substrate show the typical absorption band of silk fibroin, before and after treatments.

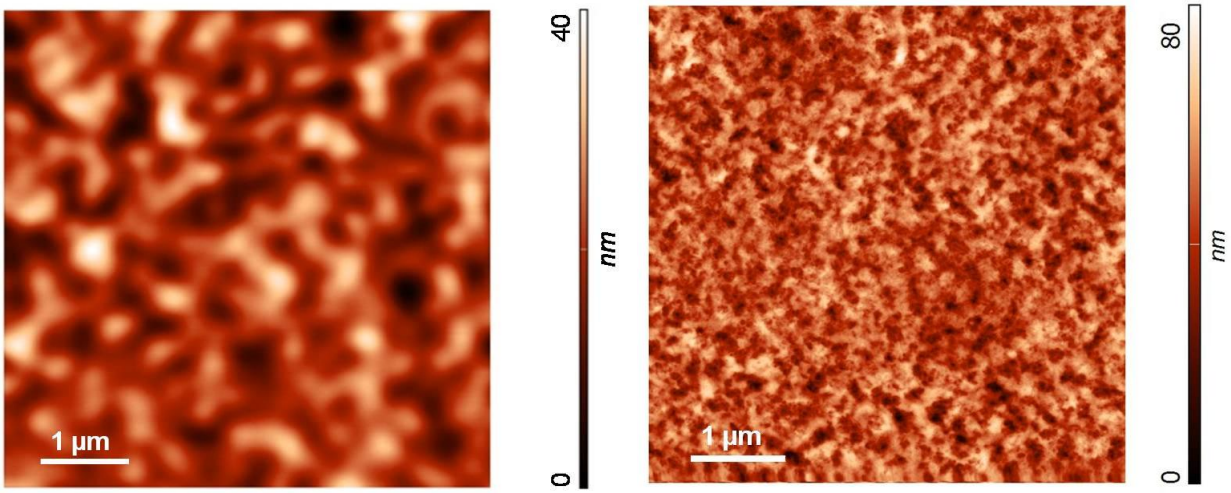

Figure S3. Tapping mode AFM image (size: 5 µm × 5 µm) of HC-PEDOT:PSS spin coated on bare glass (left side, RMS = 6 nm) or SF coated glass substrate (right side, RMS = 10 nm) and successively annealed at 120°C for 20 minutes.

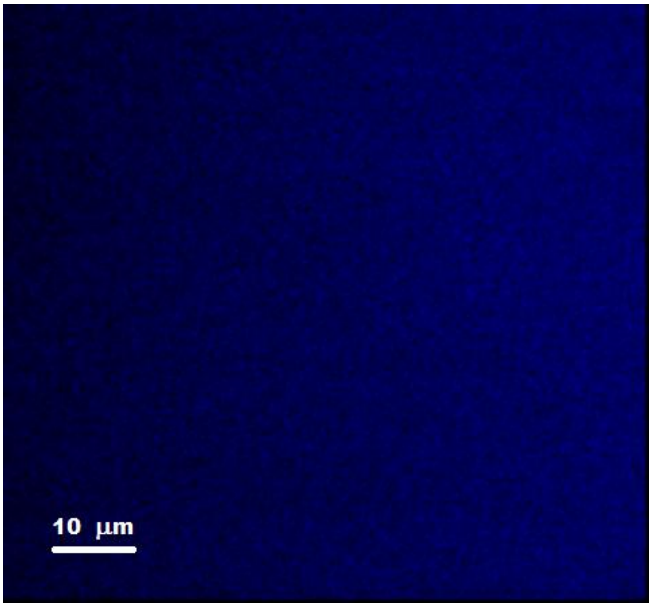

Figure S4. Confocal microscopy image (100 µm x 100 µm) of Stb dye dispersed in SF matrix (5 wt %) under continuum illumination at 405 nm with blue diode laser.

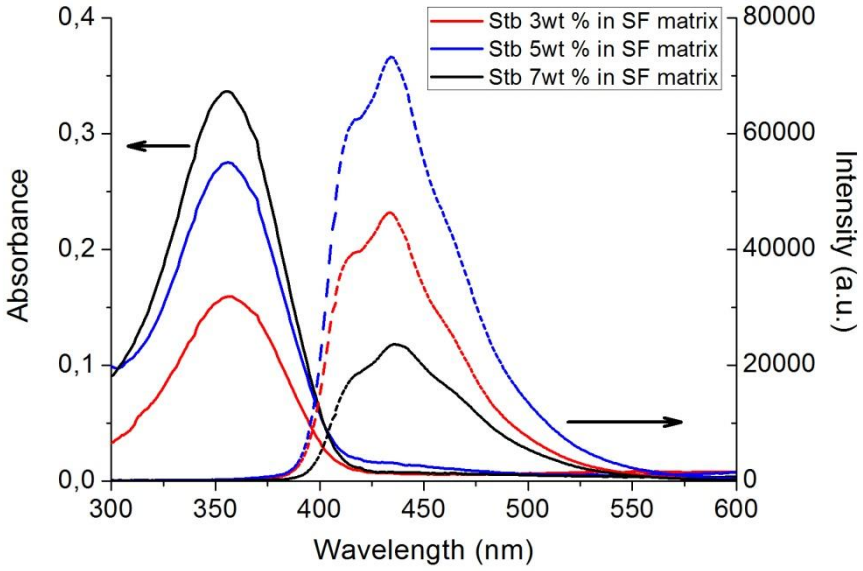

Figure S5. Absorption (continuum lines) and emission (dashed lines) spectra of Stb-SF films at different concentrations: 3wt % (red), 5wt % (blue) and 7wt % (black). For all Stb concentrations, the films show an absorption peak at 355 nm and a 435 nm peaked emission band. While absorbance increases with Stb concentration, emission intensity doesn't follow the same trend probably due to the formation of weakly emissive aggregates. As a consequence, the highest emission intensity is obtained for the SF film with a Stb concentration of 5 wt %.

Table S2. Luminescent quantum efficiencies of Stb in SF matrix for different concentrations.

Stb concentration in SF matrix (wt %)	Quantum yield (%)
3	60
5	64
7	52

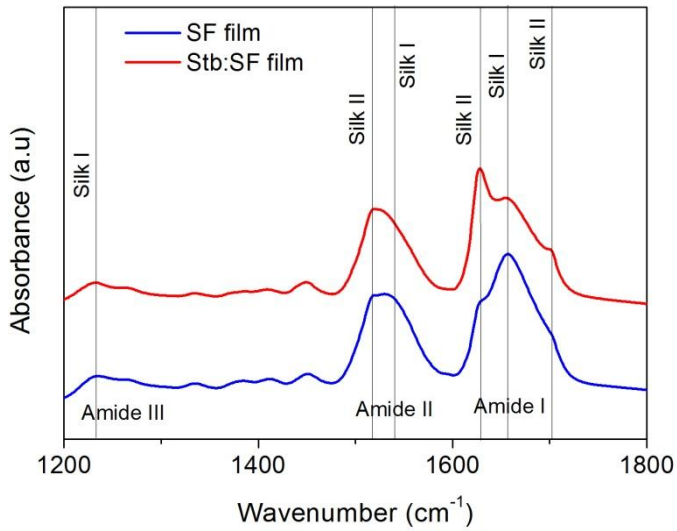

Figure S6. FT-IR spectrum of pristine (blue) and Stb-doped (red) insoluble SF films on silicon substrates.

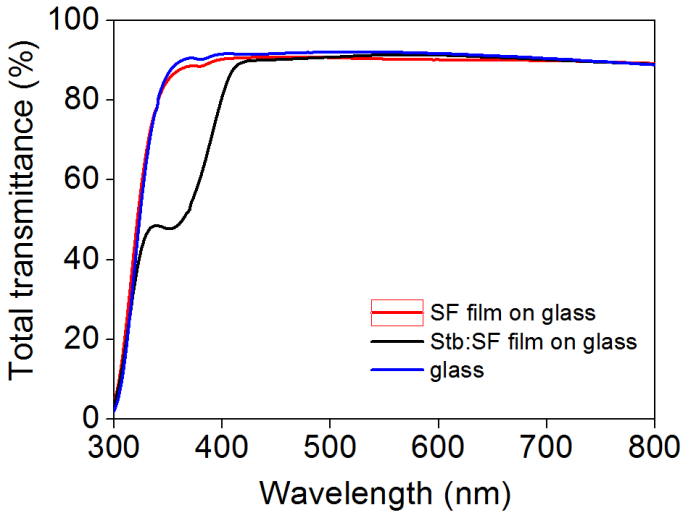

Figure S7. Transmission spectra of glass (blue), pristine (red) and Stb-doped (black) insoluble SF films on glass substrates.

Table S3. OPV performance of ITO-free P3HT:$PC_{61}BM$ based solar cells fabricated on PET or PET/SF substrate. The reported data are averaged over 5 devices.

OPV device structure	**J_{SC}** [mA/cm^2]	**V_{OC}** [V]	**FF** [%]	**PCE** [%]
PET/**HC-PEDOT:PSS**/P3HT:$PC_{61}BM$/LiF/Al	7.2	0.54	60	2.3
PET/**SF/HC-PEDOT:PSS**/P3HT:$PC_{61}BM$/LiF/Al	7.0	0.54	58	2.2

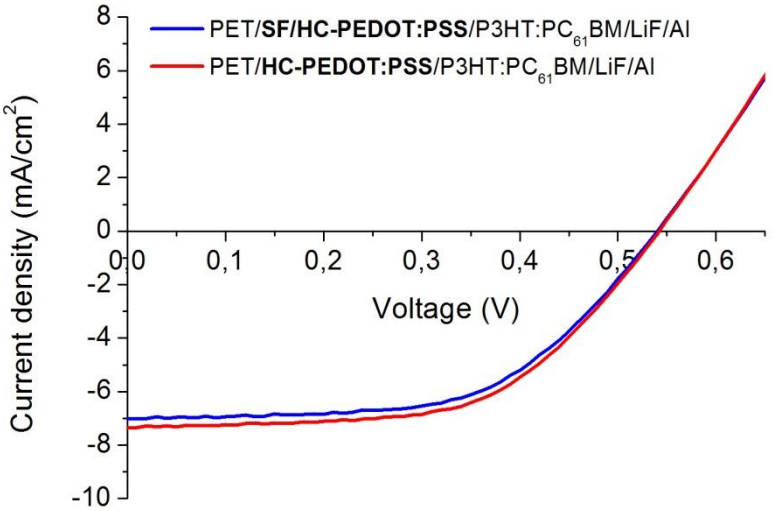

Figure S8. J-V plot, under standard illumination, of BHJ solar cells employing the structures: PET/PEDOT:PSS/P3HT:$PC_{61}BM$/LiF/Al (red trace) and PET/SF/HC-PEDOT:PSS/P3HT:$PC_{61}BM$/LiF/Al (blue trace).

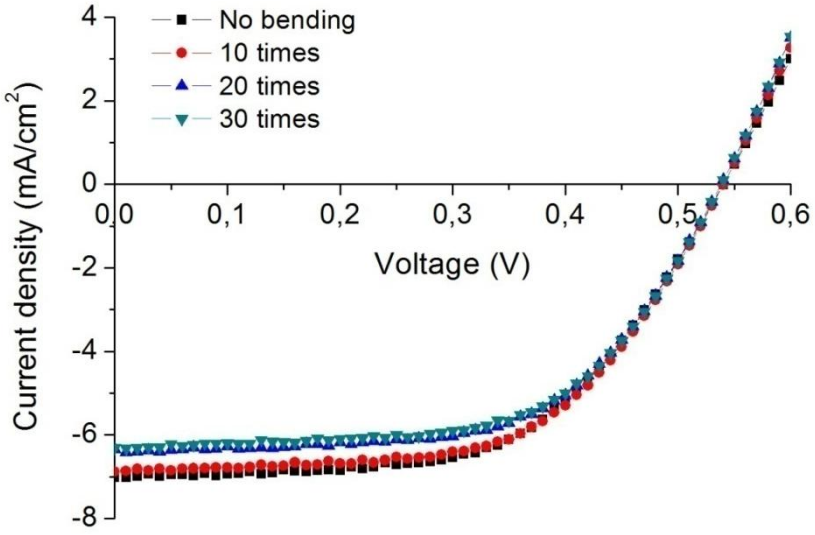

Figure S9. J-V plot, under standard illumination, of ITO-free BHJ solar cell employing the structure PET/SF/HC-PEDOT:PSS/P3HT:$PC_{61}BM$/LiF/Al after 0 (black), 10 (red), 20 (blue), 30 (green) bending cycles at a radius of ~ 10

mm. All the samples were subjected to manual bending, with cycles having a duration of 5 seconds each, in continuous mode.

Table S4. OPV performance of P3HT:$PC_{61}BM$ based solar cells using different device structures and active layer thicknesses. The reported data are averaged over 5 devices.

OPV device structure	**Active layer thickness (nm)**	**J_{SC}** [mA/cm^2]	**V_{OC}** [V]	**FF** [%]	**PCE** [%]
Device C	350	7.7	0.56	59	2.6
	100	5.0	0.55	55	1.5
Device D	350	7.7	0.56	59	2.6
	100	5.1	0.55	54	1.5